From superconductor stability and relaxation to Andreev reflections

Harald Reiss

Department of Physics
University of Wuerzburg, Am Hubland, D-97074 Wuerzburg, FRG
harald.reiss@physik.uni-wuerzburg.de

Abstract

How exactly can critical temperature be determined from results obtained in resistivity measurements? An unconventional approach using an electrical resistance network is presented in this paper to find an answer to this question. In a first step, a recently suggested, dynamic relaxation model is refined and extended beyond its proper applicability and competence range (superconductor stability against quench). This step addresses bending of the resistivity vs. temperature curves near critical temperature. In a second step, an alternative solution of the thermal fluctuations problem is presented. From both results, existence of a non-local, transition boundary layer can be postulated, a temperature uncertainty around critical temperature. Finally, severe limitations to calculate total current through superconductor/normal conductor thin film junctions become obvious from this approach if any non-Ohmic contributions (like Andreev reflection or Josephson currents) have to be taken into account. This problem is a parallel to multi-component heat transfer.

Keywords
Superconductor; phase transition; relaxation; critical temperature; cell model; thermal fluctuations; Andreev reflections; multi-component heat transfer: additive approximation

1 Superconductor stability

A superconductor is stable if it does not quench. Quench can be avoided by application of stability models to design, manufacture, handling and operation of superconductors.

Traditional literature has analysed the superconductor stability problem since the 1980s using analytical models, mostly with worst case assumptions, uniform materials properties, uniform conductor temperature and critical current density. With only few exceptions, stationary states are standard conditions in traditional stability calculations. Traditional stability models are described in [1 - 3].

Numerical methods have been suggested by the present author [4 - 8]. The results improve reliability of stability predictions. Transient, *local* materials and transport properties are in the foreground.

A recently suggested "microscopic stability model" [7] has provided the core of the numerical stability calculations. The present paper refines this model to investigations going beyond the proper stability problem. Reference is made to spatial structure of Cooper pairs, their decay to single electrons and re-condensation rates.

When [7] is integrated into a resistive cell model, the results suggest postulation of a non-local, transition boundary layer, expressed as a temperature uncertainty, ϑT_ρ, around critical temperature. Within ϑT_ρ, the resistivity curve continuously approaches the normal conduction value. Curved resistivity vs. temperature, instead of a sharp jump, is frequently observed in experiments, see Figure 1.

The results of this study, to some extent, contribute to also solution of the thermal fluctuations problem. They further open a new perspective of how current flow across superconductor/normal conductor thin film interfaces by Andreev reflections and by other non-Ohmic contributions have to be taken into account. Andreev reflections and Josephson

currents may seriously question description of current flow as a transport process. As will be shown, this is a problem similar to multi-component heat transfer in case of radiative contributions.

Finally, the transition boundary layer, ϑT_ρ, questions existence of a sharp, uniquely defined critical temperature.

The analysis described in the next Sections is focused on calculation of the resistivity of NbTi, YBaCuO 123 and BSCCO 2223 superconductors. Thin films of YBaCuO 123 with different transport properties are switched in series (Figure 2a,b).

2 Relaxation

The literature reports magnetic relaxation measurements to determine pinning potentials, like in Nb_3Sn, in the BSCCO family and in MgB_2/Fe superconductors. In contrast to these studies, focus of the stability model [7] is on relaxation of the electron system from *disturbances*, usually the origin of a quench.

We do not address *statistical* electron pair decay and recombination in dynamical equilibrium. These relaxations, at any temperature $T > 0$, exist without disturbances. Instead, the paper is focused on electron pair decay and re-condensation after temporal disturbances. This problem becomes most interesting if the electron system is already close to the superconducting/normal conducting phase transition.

The question is whether relaxation rates after disturbances are large enough to re-organize stability against quench to a new thermodynamic equilibrium. The residual, dynamic number of electron pairs after a disturbance might not be sufficient to support zero-loss (critical) current.

Superconductor stability against quench thus is an aspect of the relaxation problem.

Analysis of relaxation requests calculation of relaxation time and relaxation rates. Critical current density after a disturbance neither is uniform in the conductor cross section nor is it constant in time, compare [4 - 8] and further references cited therein. Critical current density is zero if the superconductor cannot relax As a consequence, relaxation time and relaxation rate, too, not necessarily would be uniform and constant in time.

2.1 A short recapitulation

Excitations disturb dynamic equilibrium between (i) decay of electron pairs, (ii) statistical, single electron (quasi-particle) generation rates and their recombination. Relaxation of the superconductor electron system from an excited state to a new dynamic equilibrium usually is expected to follow an exponential decay law, $\exp(-t/\tau)$, with τ the relaxation time.

In standard literature, relaxation time, τ, is considered as constant. But relaxation cannot be completed instantaneously. It is more realistic to calculate relaxation time as a sensitively *time-dependent* quantity because of its strong dependence on temperature, $\tau = \tau[T(t)]$. This step has been realized in the stability model [7].

This model is a multi-physics approach using analogues between relaxation in superconductors with re-organisation processes in nuclear and multi-particle physics.

Relaxation does not mean recombination of a strictly *limited number* of single electrons (a finite number of decay products from a disturbance) to electron pairs but re-organisation of the *total* electron body, i. e. of all electrons as far as they are "available".

Available means: The percentage of electrons, the active ("busy") part of the total body, all at states below Fermi energy, that contributes by

(i) electron pairs, in dynamic equilibrium with
(ii) single electrons

to thermal and electrical transport. This fraction is indicated in the literature, for low-T_C and high-T_C superconductors, as roughly 0.1 and 10 percent of the total body, respectively (these are rough estimates taken from the energy to energy gap ratio). Exact, experimental data of these percentages cannot be found.

Item (i) of the above: When electrons combine (relax) to an electron pair, one electron is provided from energetic states slightly above the Fermi sea, the other electron belongs to bound states located below this level. After an excitation (a few meV) that they need to cross the energetic gap, both electrons, as a pair, plus the residual, uncoupled, (single) electrons all constitute the active part and contribute to electrical current (thermal energy transfer, however, relies on only the single electrons).

Electrons from the inner core (strongly bound states, the inactive part) of the total electron body would request much higher than meV-energies and thus cannot be excited to form electron pairs.

The Ginzburg-Landau order parameter, $f_S = n_S(T)/n_S(T=0)$, *within the active part,* then determines the number of electron pairs available for zero-loss current.

Order parameter and all steps of the relaxation process have to strictly follow selection rules, among these in particular the "Coefficients of fractional parentage" (cfps), a concept applied in atomic and nuclear physics, and the Pauli exclusion principle.

Item (ii): This contribution can be neglected from thermal and current transport against the favourable transport properties of, item (i), the active electron system.

Calculation of the order parameter by the model [7] follows a step-wise procedure prescribed by the definition of the cfps: Each available electron, in a statistical approach, one after the other among all, has to find its (appropriate) partner to form a pair. "Appropriate" means: In conformity with selection rules.

The order parameter, $f_S = n_S(T)/n_S(T=0)$, with $n_S(T)$ the strongly temperature dependent density of electron pairs, is shown in Figure 3. It is calculated by application of [7] to NbTi, YBaCuO 123 and BSCCO 2223 superconductors. Obtained relaxation time, τ, and relaxation rate, $\xi = \Delta f_S/\Delta t$, are shown in previous publications [7, 8]. In all investigated cases, the most remarkable result is the divergence of the relaxation time, τ, near T_{Crit}.

2.2 Discussion of alternatives

Contrary to the *stepwise*, cfp-controlled procedure [7, 8] (see also **Additional explanations 1**), an analytic, continuum expression for the electron pair density can be found in Eq. (8) of [9], with $n_S(T)/n_0 = 1 - (T/T_{Crit})^4$ and n_0 the total number of electrons at T = 0.

But this expression neglects the dynamic aspects of the relaxation problem. It does not explicitly integrate the step-wise sequence of a large number of *single*, statistical, quasi-particle generation and recombination processes. Eq. (8) in [9] implicitly assumes *simultaneous* re-organisation of the decay products to a new, recombined set of electron pairs and single particles; it does not consider this process as a *sequence* to restore the whole electron system to a new dynamic equilibrium.

In correct calculation, the re-organisation has to include, for each electron, n, that "looks" for its partner, n', to form a pair, the calculation of its *own* cfps (coefficients of fractional parentage) from the *previous* N - 1 completed re-organisations. This means it requests expanding the wave function of a new, completed recombination state (N) (with the wave functions composed of single particle states) in terms of

(j) the foregoing expansion of the (N - 1)-state and
(jj) incorporating the wave function of the new pair (n, n') into the state N.

Step (j) is necessary to observe the Pauli selection rule. Eq. (8) of [9] also violates this principle.

Fortunately, both the direct (stepwise, microscopic) method [7] and, with some additional assumptions, the apparently heuristic Eq. (8) in [9], allow calculation of relaxation rates and relaxation time.

While the differences obtained for the order parameter (and, as a consequence, also for the relaxation rates) at temperature significantly below T_{Crit} are substantial (Figure 3, and Figure 8a of [21], part B), order parameter and relaxation rates in both concepts [7] and [9] converge to zero when the system during warm-up very closely approaches its super-conduction/normal conduction phase transition.

Relaxation time, as is shown in [7] and in Figure 11 of [21], Part B, increases the more the closer the electron system during warm-up approaches its phase transition.

This conclusion is in conflict also with Buckel and Kleiner [10], Chap. 4, p. 262. The authors state that in conventional superconductors the probability that an unpaired electron finds a suitable partner for recombination to form a Cooper pair decreases under increasing temperature. But the present situation, relaxation from disturbances, is strongly different. This can be seen as follows:

Starting from an original, dynamic equilibrium at a temperature, T, followed by a disturbance at this temperature (leading under continued warm-up to temperature T' > T), increasingly *more* single particles, n(T'), n'(T'), have to recombined to pairs in order to generate, by reorganisation of the *total* electron body, N_{Total}, a new dynamic equilibrium at T'. This statistical, un-displaced dynamic equilibrium, as one step out of a great

number of analogue ones, like all others can be obtained only if relaxation has been completed at each of the temperatures, T'.

Contrary to [10], an increased number, n(T') > n(T), of single electrons *within* the total body, $N_{Total}(T')$, has to be reorganised to pairs, which means, a larger number n(T') of single electrons, as decay products, has to identify partners, n'(T'), under observation of the said selection rules (cfps and the Pauli principle). Each of these numerous identification (and corresponding re-organisation) steps takes non-zero time intervals (compare [7] for the estimate). Accordingly, relaxation time *increases* the more strongly, the more closely temperature approaches T_{Crit} (reversely, relaxation time decreases with decreasing temperature).

As another potentially alternative, explanations suggested in the original papers by Gray et al. [11,12] do not refer to a temperature increase from absorption of a radiation pulse or from other thermal disturbances. Contrary to the situation described in [7], the papers [11,12] describe *injection* experiments to create an *additional* number, Δn, of quasi-particles *above* the "core" (N) of bound electrons in the undisturbed superconductor. This does not take into account the cfp-rule that must be observed *within* the $N_{Total}(T')$ state. Injection experiments, as a consequence, cannot be described by the model [7].

The model [7] therefore contradicts [10] (but is not contradicted by this reference), because the balance to yield N in [10] is not complete, and it also contradicts [11, 12] (but is not contradicted by injection experiments) because additional electrons are not delivered in [7] to the previous state (the number of electrons under warm-up remains constant, except for extremely high temperaturess).

The conclusion from [7] also specifies a note that Annett [13], p. 52, added to the left column of his book. There we have: "The word superconductor is used only to mean a material with a *definite* phase transition and critical temperature." (correction by the present author: "definite", here written in Italics, probably means "completed"). But critical temperature is a dynamic, *equilibrium* electron state unto which a series of *non-equlibrium* states may converge when *no more disturbances*, besides statistical fluctuations, have to be compensated.

Another item to be explained is determination the spatial structure of Cooper pairs in a superconductor volume. It is widely accepted in the literature that a number of in the order $N = 10^6$ to 10^7 Cooper pairs overlaps within one, specific electron pair.

It is not correct to assume, as has been made in [14], that the Cooper pairs occupy a specific superconductor volume element (or the volume of a single Cooper pair) in that they fill these volumes uniformly and that magnetic field lines would penetrate this volume in-between neighbouring (overlapping) electron wave functions. A magnetic field would not penetrate the superconductor by just single field lines but by vortices (anything else violates conservation of energy). Even under large magnetic fields, distance between neighbouring vortices, and thus between electron pairs, as long as the critical field is not exceeded, does not become zero.

A more attractive explanation of the spatial structure of Cooper pairs, directly from BCS-theory, is provided in [15]. This paper describes a real-space structure of the electron pair distribution by symmetrical, quasi-atomic wave functions. The Cooper pairs in this model constitute an

identical, spherically layered structure (the author [15] speaks of "onion-like"), for each of the electrons forming a single Cooper pair.

Spatial charge modulation of the spherically layered structure in [15] is reflected by a corresponding charge modulation of the background ionic lattice. A first question then is whether the lattice could follow quickly enough charge modulations within the electron pair foreground. A second question concerns spatial structure of the electron pairs:

Electron pairs cannot be regarded as minute, *materials* entities. Instead, they are just *relation*s between electrons j and k, with the j and k continuously exchanged, which means replaced by other electrons that randomly (under observation of quantum-mechanical selection rules) are selected from a very large number (within the active electron body) of single electrons. The selection and recombination processes simulated in [7] all are statistical ones.

Yet the explanation [15] of the spatial structure of electron pairs will tentatively be applied in Sect. 3 to derive a "pseudo-porosity" (like the porosity of a solid or liquid) of the superconductor as a function of the order parameter. This model is restricted to current within solely the electron body. As will be shown, the porosity separates, in dynamic equilibrium, residual Cooper pairs from single (residual) electron states. While this approximation appears to be acceptable, at least for a tentative approach, the next problem arises from the idea that current across a superconductor/normal conductor interface could be described as a "transport process". Which specific properties get a process a "transport" process? We will come back to this question in Sect. 6.

3 Curvature of resistivity vs. temperature

The literature reports a great number of electrical resistivity, $\rho_{El}(T)$, or of conductivity, $\sigma_{El}(T)$, curves with remarkable deviations from the expected, sharp increase of $\rho_{El}(T)$ of decrease of $\sigma_{El}(T)$ at T_{Crit}.

We make an attempt to explain the observed rounding of the transition curves by a correlation with variations of the superconductor order parameter within a two-component, resistive cell model.

Glover III [16] claims evidence that the observed rounding of $\sigma_{El}(T)$, the "thermal fluctuations problem", in thin samples with short electron mean free paths relies on an intrinsic materials property, a "sort of fluctuating superconductivity".

The cell model described in the following does not rely on *fluctuations* of superconductivity (it is not very clear what is really meant by fluctuations around/between what, and to which extent). The model instead relies on calculation of an effective resistivity or conductivity of two *phases* existing in parallel in the superconductor (residual, normal conducting, single electrons and condensed, superconducting electron pairs; the model is similar to a two-liquid model).

In contrast to [16], there is no fluctuation *within one* but variable contributions by *two* phases. Under dynamical equilibrium, their contribution to effective electrical resistivity relies solely on a function of the order parameter. This parameter is a unique, strong function of temperature. Temperature may fluctuate locally, e. g. under non-uniform materials properties. Non-uniform temperature distributions have been simulated in our previous papers.

The two-fluid model in the following applies a resistance network. Two-fluid models are well known from standard superconductivity literature and from thermal physics and fluid dynamics. Description of the effective resistivity of this network is given in terms of a porosity (to be defined clearly). The porosity is based on the order parameter and its temperature dependency.

3.1 The resistive network

The cell model applied in the following does not address random distributions of superconducting and normal conducting *volume* elements (spherical, cubic or of other geometry) obtained from random, local variations of T_{Crit} (this would be similar to Finite Elements meshing). While also such distributions allow definition of an effective conductivity or resistivity, we instead consider, *within* any volume element of arbitrary size, the distribution of super- and normal conducting phases.

The Russell cell model [17] is a standard tool for application to two-component systems to describe their effective materials and transport properties. It was originally derived for thermal, solely conductive transport but applies to also electrical, in general to any conductive transport process provided it (i) is really a "transport" process and, if so, can (be expressed (ii) by a differential formalism (like in Fourier's differential equation in case of solely conductive heat transfer).

Network and cell model will be applied first to the region $T < T_{Crit}$ (extension to $T > T_{Crit}$ will be made in Sects. 4 and 5). Let k_{Core} denote, in traditional application of this model, thermal conductivity of spherical "inclusions" completely embedded in a continuum (a matrix or "Shell", like in an open cellular structure).

In a thermal super-insulation, for example, the inclusions in the evacuated space are minute, solid particles (powders or fibres). The thermal conduction (if it exists, this is not trivial, see Sect. 6.3 or [21, 22]) of the surrounding continuum (if it is the vacuum) is given by its residual gas pressure. If k_{Shell} denotes thermal conductivity of the Shell, the ratio k_{Core}/k_{Shell} in thermal super-insulations is very large.

The procedure is applicable to any other continuum, not only to evacuated space filled with solid particles.

If porosity, Π, is known, the effective, integral conductivity, k, according to the Russell cell model reads

$$k = k_{Core}\,[\Pi^{2/3} + (k_{Core}/k_{Shell})\,(1 - \Pi^{2/3})]/[\Pi^{2/3} - \Pi + (k_{Core}/k_{Shell})\,(1 - \Pi^{2/3} + \Pi)] \qquad (1)$$

and applies to also resistivity when k is replaced by $\rho = 1/k$.

In its original formulation, the Russell cell model describes thermal conduction heat transfer in a solid (brick) with pores, all of the same size and of cubic or spherical geometry (the effective conductivity of a hypothetical reverse case, i. e. shell replaced by core, could be calculated from Eq. (4) by interchanging Π by 1 - Π).

In order to apply the Russell cell model, or any other traditional cell model, not only to powders, fibres or porous solid structures but to also *superconductors*, the "inclusions" have to be interpreted as being composed of sets of electron pairs, and the "shell" is given by an overwhelming number of single electrons (decay products arising from disturbances), all with small electrical conductivity, under dynamic equilibrium in the active part of the total electron body.

To get this working, we have to define a corresponding "pseudo-porosity", Π, in terms of the distribution of active and inactive parts of the electrons.

With increasing temperature, the number of "inclusions" (sets of electron pairs) goes to zero at the phase transition; the porosity of the total, then normal conducting (NC) electron body approaches Π = 1. The resistivity of this state, a finite value, $\rho_{El,NC}(T)$, can be obtained from experiments.

Electron pair, *zero* resistivity, $\rho_{El,Core} = \rho_{El,SC}(T)$, on the other hand, cannot successfully be applied in Eq. (1). It has to be represented by a finite, *non-zero* resistivity, $\rho_{El,Core} > 0$. This (pseudo-) resistivity of the superconducting, transport channel by electron pairs, if it exists at all, must be smaller, by many orders of magnitude (at least 20), than the resistivity of the normal conducting phase, the shell.

The ratio 20 is not the real problem; instead, it is the "existence" of resistivity or conductivity components. "Existence" of *all* resistivity or conductivity components must have been assumed in [10], Eqs. (6-8) and (6-9). This very complex situation shall be clarified in a critique presented in Sect. 6.3. The critique is based on an analogy of this problem to "existence" of total thermal conductivity or resistivity in multi-component heat transfer if one of the components (radiation) cannot be described as a conductivity, like in thin, partly transparent films.

The ratio $k_{El,Core}/k_{El,Shell} = \rho_{El,Shell}/\rho_{El,Core}$ in Eq. (1) is defined only under the assumption ($\rho_{El,Core} > 0$).

Predictions of the cell model may diverge at very small and very large values of the porosity (this is a weak point of all cell models). Application of this model to superconductors thus might become critical when, under warm-up, the number of electron pairs near T_{Crit} goes to zero so that the porosity approaches $\Pi = 1$. In a control calculation, the resistivity must converge to the finite value $\rho_{El,Core}$. If this the case, the cell model provisionally appears to be applicable to the present problem. This can easily be checked by assuming $\Pi = 1$ in Eq. (1).

For Figure 2b, a finite non-zero resistance originating from weak links would request incorporation of another rectangle, but is neglected in this presentation (its contribution shall be enclosed in the blue rectangles).

Figure 6a-c of [4] apparently was the first application of a cell model, again the Russell cell model, to a superconductor.

3.2 Calculation of the pseudo-porosity

The pseudo-porosity, Π, must be defined precisely. Porosity in the following has to be explained as a function of the ratios by which electrons, in their two conducting phases, contribute to total electrical conductivity. Contribution of the phases is solely related to temperature dependence of the ratio of particle density at temperatures T and T_0 (T_0 taken as a reference value). This ratio is given by the Ginsburg-Landau order parameter, $f_S(T)$.

Using n_S for density of electron pairs, and since n_S depends strongly on temperature, the fraction $1 - f_S$ needed for derivation of the porosity, cannot be constant, which means the pseudo-porosity, too, is a function of temperature.

The number, N_{CP}, of Cooper pairs in an arbitrarily, small volume, V_{SC}, of the superconductor material is given by

$$N_{CP} = f_S(T)\, n_S(T_0)\, V_{SC} \qquad (2)$$

The distance of two electrons forming a Cooper pair can be approximated by the coherence length ξ, about 10 nm in both BSCCO 2223 and YBaCuO 123 superconductors; in NbTi, ξ taken from [10] is 5.8 nm. Spatial size of one Cooper pair (as mentioned, not a materials volume), within which *correlation* between two electrons exist, is dV_{CP}. The total correlation volume, V_{CP}, of *all* Cooper pairs N_{CP} in the volume V_{SC}, in a rough approximation, results from $V_{CP} = N_{CP}\, dV_{CP}$. A number of about $M = 10^6$ to 10^7 pairs overlap to an effective, spherical correlation volume [15] within V_{SC},

$$V_{CP,eff} = (N_{CP}\, dV_{CP})/M \qquad (3)$$

from which the porosity

$$\Pi = 1 - V_{CP,eff}/V_{SC} \qquad (4)$$

With increasing temperature, $T \rightarrow T_{Crit}$, the number N_{CP} decreases, which means the porosity increases, $\Pi(T) \rightarrow 1$, and the resistivity $\rho_{El}(\Pi)$ converges, in a steady transition, to the normal conducting value, $\rho_{El}(T) \rightarrow \rho_{El,NC}(T)$, compare Figures 4, 5 and 6a,b. This is important and even favourable (still under the proviso for applicability of the cell model): The resistivity does not diverge to un-physically large numbers.

At T very close to T_{Crit}, handling of the procedure collides with limitations set to the applicability of Fortran routines or of Excel sheets. When declaring real and integer variables as "Real*16", the smallest possible deviation that can be simulated, $T - T_{Crit}$, is 10^{-16} K. This sets a limit to the porosity obtainable from Eqs. (2) to (4).

Accordingly, a numerical set of porosities is generated, the individuals of which converge to the pure, normal conduction resistivity. Figure 4 shows resistivity, $\rho_{El,Core} = \rho_{El,SC}(T)$, of YBaCuO 123 as function of porosity, and Figures 5 and 6a the resistivity of NbTi, YBacuO 123 and BSCCO 2223 vs. temperature.

Detailed inspection of the diagrams in Figure 6a confirms the deviation from a sharp jump of $\rho_{El}(T)$ at $T < T_{Crit}$. The deviations become more obvious in Figure 6b (enlarged sections of $\rho_{El}(T)$ of the NbTi, YBaCuO 123 and BSCCO 2223 resistivity diagrams) and in Figure 6c for the electrical conductivity of the BSCCO superconductor.

As was to be expected, the more temperature approaches T_{Crit}, the larger, trivially, is the contribution in the Russell model to $\rho_{El}(T)$ by the normal conducting phase, $\rho_{El,NC}(T)$. This means the temperature dependence of $\rho_{El,NC}(T)$ increasingly determines the excursion with temperature of the total resistivity, $\rho_{El}(T)$.

3.3 Symmetry operations

Can we extend the results from Figures 5 and 6 a-c to $T > T_{Crit}$, in an attempt to generate the full curve, $\rho_{El}(T)$, over the total temperature scale? The attempt will be restricted to $T_{Crit} - 2\ K \leq T_{Crit} \leq T_{Crit} + 2\ K$. This result shall be transferred to Sect. 4 to suggest existence of a tentative,

new explanation or at least a contribution to understanding of the thermal fluctuations problem (the full curves in Figure 6a are already obtained from point-symmetry operations described in the following).
For this purpose, we divide the plane $\rho_{El,SC}$ vs. T in Figure 5 into 4 quadrants and map the curve $\rho_{El,SC}(T)$ from quadrant 4 to quadrant 1 by three, successively performed symmetry operations. Details are reported in the Appendix (see Figure 9).

These symmetry operations are justified because they are applied to *solely* the superconductor electron system, $\rho_{El,SC}(T)$, not to the lattice with its zero electrical conductivity. The operations are justified also because they are restricted to the small temperature interval within which the resistivity from zero increases to large values.

From Figure 6b, a (non-local) boundary layer, δT_ρ, can be identified within which this increase, near critical temperature, is completed; see Sect. 5 for the width of this boundary layer.

This interval *solely* results from the symmetry operations described in the Appendix. Width of this interval depends on the sensitivity by which $\rho_{El,SC}(T)$ decays from $\rho_{El,NC}(T)$ when temperature is slightly reduced below T_{Crit}.

An interesting question is whether the derivation of the interval δT_ρ could be applied to also the extent of the proximity effect, but this needs separate investigations.

4 Application to the Thermal Fluctuations problem

While the behaviour of the calculated $\rho_{El}(T)$ in Figure 6a-c qualitatively confirms bending or resistivity vs. temperature curves frequently seen in standard experiments, the deviations of the calculated curves seen in relation to their measurements, that in particular are observed in regions corresponding to ellipse I in Figure 1, are much larger. Strong deviations from the expected sharp jump were observed in particular during early stages of HTSC development.

The reason for the deviations from sharp increase may be manifold: First, a straight, vertical line, at exactly $T = T_{Crit}$, could be observed only in case composition of the material is absolutely stoichiometric and perfectly clean. This is presumably the most important source of uncertainties like bending. Trivially, derivation of the pseudo-porosity (and its definition) might be erroneous, or the whole cell model might not be applicable at all to superconductors (but the results appear plausible). But also measuring the curve $\rho_{El}(T)$ at temperature very close to T_{Crit} is (potentially) extremely difficult, with possibly large uncertainties.

In any case, the explanation of the deviations from the experimental curves in Figure 1 is not a "phenomenon" (a rather generous classification frequently found in the literature; it sounds as if a situation cannot be understood). Instead, it appears it is simply the physical consequence of the strong temperature dependency of the order parameter (and the weak temperature dependence of the normal conduction resistivity).

In the reverse situation, during cool-down from $T >> T_{Crit}$ to T_{Crit}, the smaller T, the smaller is the contribution to the effective resistivity by the normal conducting electrons, and thus the smaller is the total value.

5 Consequence for unique definition of T_{Crit}

The boundary layer is not a materials layer but, in the $\rho_{El}(T)$-diagram, a small temperature interval within which resistivity changes drastically. This region can be interpreted as a temperature uncertainty δT_ρ that exist *throughout* the superconductor material; the layer does not separate superconducting from normal conducting, *local* materials regions. The curve steadily approaches the convergence limit (and even can be differentiated).

This is in analogy to *local* temperature boundary layers, δT, well-known from thermal, in particular from radiative transfer and from local δv in fluid dynamics. However, while these layers usually occur near solid surfaces, the *non-local* resistivity layer δT_ρ is not associated with a solid boundary nor does it belong to a specific materials section. Existence of δT_ρ in the end results from the temperature dependency of the order parameter.

It is thus within the temperature interval, δT_ρ, in Figure 6b (and, correspondingly in the conductivity) that T_{Crit} cannot be defined sharply.

Besides conclusions drawn from solely the microscopic stability model, Figure 11 in [21], part B, on whether T_{Crit} can be defined uniquely in view of the diverging relaxation time (recall **Supporting Information 1**), this is the second argument to question not only its sharp *definition* but even the mere *existence* of a uniquely defined critical temperature in superconductors.

From Figure 6a, width δT_ρ of the boundary layer is between 11 (NbTi) and 20 (YBaCuO and BSCCO) µK, for decay (within δT_ρ) of ρ_{El} by 1.68 e-6,1.11e-5 and 1.22e-5 Ω m, respectively. This yields gradients, on the average, $\Delta\rho_{El}/\delta T_\rho$ = 0.153, 0.557 and 0.610 Ω m/K for NbTi, YBaCuO and BSCCO. The gradients (or their reverse values) allow estimates of the uncertainty by which critical temperature can be determined from resistivity (transport) measurements in these materials.

Reduction of the width δT_ρ would be interesting to isolate T_{Crit} with reduced or even without uncertainty. A reduction of δT_ρ could possibly be found on the basis of correlations between T_{Crit}, J_{Crit} and relaxation. Such correlations do exist, compare Figure 5a,b in [18]. But it is presently not clear whether a correlation between these critical parameters *and* the uncertainty δT_ρ could be demonstrated.

6 Limitations of the cell model

6.1 Specification of current flow as a transport process

Andreev reflections like Josephson currents are responsible for current flow in parallel to current transport across Ohmic resistances (see standard volumes on superconductivity). In the literature, Andreev reflections usually are explained at solid/solid contacts between super- and normal conductors.

Discussion of Andreev reflections in the following is not restricted to solid/solid contacts between materials of different composition and transport properties. Instead, several thin films built up to a stack may be composed of the *same* superconductor material, with the films in different thermodynamic state, here simulated by different values of the

pseudo-porosity, Π, or the order parameter, within the cell model. This procedure is just to simplify the following simulations.

Different values of Π trivially result from disturbances that drive the superconductor at local positions from superconducting (SC) to normal conducting (NC) state. Local fluctuations of materials properties may do the same job: Variations of thermal diffusivity or of refractive index, strictly speaking of all obstacles to conductive and radiative transfer in solids and thin films (examples are shown in Figures 6a,b and 7 in [19]).

The impact of temperature fluctuations or of fluctuations of electrical resistance accordingly is reflected by the order parameter.

Ohmic current in the following is modelled as a current *transport* process across several resistances. Transport processes in general are initialized under potential differences or potential gradients.

Contribution of Andreev reflections to total current in parallel to Ohmic current is given by a net transport rate of 2e charges across the SC/NC interface; this contribution not necessarily requests an electrical potential difference, U. The contribution by Josephson current follows from Josephson equations 1 and 2. DC Josephson currents are observed in case U = 0.

Therefore, while Andreev reflections, too, contribute to total current, they like Josephson currents cannot be simulated in a resistive cell model as a proper transport process.

6.2 Specification of the simulation scheme

Simulation of total current including Andreev or Josephson contributions requests at least two layers, a superconductor (layer 1) in solid/solid contact to a normal conductor (layer 2). We additionally assume an interfacial layer between both (see Figure 7), this shall simulate the proximity effect (and it is practical since it allows to first describe a standard SC/NC/SC sequence without modifications of this Figure). Thickness of the sequence SC/NC/NC (then counted as layers 1 to 3) is large against electron mean free path which in turn is large against coherence length (values of the thickness are given in Captions to Figures 7 and 8).

In this Section, we use "SC" and "NC" instead of the traditional "S" or "N" identifications in semi- or superconductor literature. The point is: We consider super- or normal *conductivity* states within, for simplicity, the *same* superconductor material instead of super- or normal *conductors* (superconductors contacting normal conductors like in SNS junctions).

We also assume temperature as identical in the three layers, again for simplicity. Layer 1 is assumed as SC. In the cell model described in the foregoing Sections, this means its porosity is $\Pi_1 < 1$.

Layer 2 (the interfacial layer) separates layer 1 from the normal conducting layer 3 under solid/solid contacts. Properties of the interfacial layer are simulated by a porosity gradient, $d\Pi_2(T)/dT$.

With the cell model, we have $\Pi_3 = 1$. Since Π depends on the order parameter, it is clear that $\Pi = \Pi(T)$ in all three layers. At any given temperature, $\Pi_1 \leq \Pi_2 \leq 1$.

For simulation of the Ohmic current contribution to total current, we apply the resistivity from Figure VII - 11 in [20]. The values, $\rho_{El}(T)$, of YBaCuO 123 have been extrapolated linearly from the region $T > T_{Crit}$ to T_{Crit} - 2 K $\leq T \leq T_{Crit}$, see the green solid line in Figure 1 (an analogue applies to the other superconductor materials). Strong deviations from the linear relationship would be expected only at $T << T_{Crit}$.

The extrapolated $\rho_{El}(T)$ serve for definition of the genuine resistivity in the superconducting state. The resistivity $\rho_{El,SC}(T) = 0$ is obtained either under down-bending if $\Pi(T) << 1$ or we have, trivially, in the ideal case (no down-bending, sharp decrease) $\rho_{El,SC}(T) = 0$ at $T < T_{Crit}$. In both cases, the ideal value $\rho_{El,SC}(T) = 0$ solely results from contribution of the electron pairs to conductivity in that all normal conducting components are totally short-switched by electron pairs.

6.3 A critique initiated by a parallel to multi-component heaet transfer

Using the extrapolated $\rho_{El}(T)$ (compare again Figure 1), results obtained from the cell model for the total resistances of SC/NC/SC and SC/NC/NC contacts (Figure 8), comprise only those electrons (from the active part) that contribute by Ohmic, not by Andreev reflections or Josephson currents, to total current. This is because extrapolation of $\rho_{El}(T)$ is made from temperature $T > T_{Crit}$, where only normal conduction components of current exist, to $T < T_{Crit}$. The delicate point is: Determination of T_{Crit} is done, in countless experiments reported in the literature, by measurement of the course of *total* resistance or resistivity within small intervals around T_{Crit}.

The proper resistance accordingly must be smaller than the values shown in Figure 8.

Corrections from Andreev reflections to measured total current, *below a certain voltage limit,* at local positions like at a tip, may considerably be large, according to [10], p. 315: "as twice as large as would be expected if the electron were simply to penetrate into the superconductor." For the present problem, emphasis of this specification ("below a certain voltage limit", set in Italics by the present author) is on voltage dependency which, as a consequence, would reflect a dependency on film thickness.

This situation is similar to multi-component heat transfer. If besides solid conduction radiation contributes to heat flow, the thermal conductivity or diffusivity (if it can be defined at all) then apparently might depend on sample thickness (this is the "thickness-effect" that was discussed in the 1980s literature, but has been solved meanwhile [21, 22]).

In thermal physics, in order to define conductivity as a true materials property, the sample must be non-transparent to radiation. A sample is non-transparent to (direct) propagation of radiation if its optical thickness is large. Radiative and, as a consequence, total thermal conductivity *exist* only in this case. And only in this case can solid conductive and radiative components of multi-component heat transfer be calculated as independent of each other (as if the other component is not present) and can be separated.

The question now is under which conditions an effective, total resistivity, $\rho_{El,SC}(T)$, or its reverse, an effective, total conductivity, as a genuine materials property, in analogy to the thermal analogue, would exist,

which means, without dependency on experimental conditions like sample thickness, and if each component can be calculated "as if the other is not present" and if the components can be separated experimentally.

The question thus is: What is the analogue to radiative non-transparency that could facilitate calculation of total electrical current in terms of independent components?

In thermal physics, large optical thickness, $\tau \rightarrow \infty$, transforms the very complex integro-differential equation (the "Equation of Radiative Transfer") to a differential equation, like Fourier's differential equation. The so called "Additive Approximation" [22], which means algebraic addition of conductivities, becomes applicable under solely *this* condition.

What then is, in current flow across superconductor/normal conductor junctions, the analogue to optical thickness that would

(i) get electrical resistivity a genuine, solely *materials* property that does not depend on experimental parameters like thin film thickness
(ii) allow conductivity components to be calculated independent of each other (and experimentally be separated) and then algebraically be added to a total conductivity
(iii) describe total current flow by a differential equation?

In heat transfer calculations, summation of conductive and radiative components to total heat flux $q_{Total} = q_{Cond} + q_{Rad}$ (Ws/m^2), is correct, clearly from phenomenological viewpoints. But it is, in general, not correct to simply add corresponding conductivity components, λ_{Cond}, λ_{Rad}

(W/(m K), to a total, solid plus radiative conductivity, $\lambda_{Total} = \lambda_{Rad} + \lambda_{Cond}$. The components might be coupled by the temperature profile in a sample, which means they would not be independent of each other or even would not exist at all. This is the case within radiative heat transfer; it is not clear that a temperature gradient and thus a radiative conductivity would exist. In multi-component heat transfer, a total conductivity therefore exists only if a temperature gradient exists, which means: if temperature profile, T(x), is differentiable.

By analogy, the simple, algebraic addition of electrical current components, I_k, like the algebraic addition of the q_k in multi-component heat transfer, of course is correct, again from the phenomenological viewpoint. But the authors [10], p. 320, say, below Figure 6.8: "This means in the end that I_q (note by the present author: the quasi-particle current) is treated in terms of an Ohmic resistance R." Close inspection of Eq. (6-9) in [10],

$$I = I_j + I_q + I_v$$

using $I_q = U/R$, therefore is needed to clarify whether really *all*, not only the component I_q in this equation, can be derived straightforward from conductivities or resistances (this is hardly the case with Andreev reflections and Josephson currents) and whether they can be calculated as independent of each other.

In multi-component heat transfer, the condition "Independent of each other" means: Are the components strictly switched in parallel, not in series?

The essential question to be answered with respect to also electrical current trough thin film SC/NC junctions therefore is: Are *all* the components in Eq. (6-9) of [10] switched exactly in parallel, not in series, to each other? And can they experimentally be separated?

Since radiative conductivity does not exist in multi-component heat transfer, as a consequence both radiative *and* a hypothetical total conductivity do not exist. The same might happen when describing electrical current through thin film junctions. This situation clearly needs thorough methodological investigations.

7 Summary

Bending of the specific resistivity, $\rho_{El}(T)$, at $T < T_{Crit}$ can qualitatively be explained by a resistance model with temperature dependence of the order parameter taken into account. With this model, even the thermal fluctuations state, at least partly, can be explained. But the model will get into problems if non-Ohmic contributions to current flow, like Andreev reflections or Josephson currents across superconductor/normal conductor contacts, cannot be neglected.

Curvature of the resistivity at temperature below and above T_{Crit} suggests definition of a non-local resistivity "transition boundary layer" expressed as a temperature uncertainty interval δT_{ρ} around critical temperature. From the curves $\rho_{El}(T)$, gradients in the order of 0.1 to 1 (Ω m/K) are extracted that allow to estimate the uncertainty by which critical temperature can be determined from resistivity measurements of these materials.

Critical temperature, if it is understood as a *sharply, with zero tolerance defined* physical (thermodynamic) quantity, then would be a fiction. This

follows from (a) the microscopic stability model (the strong divergence of relaxation time) and (b) the finite temperature interval δT_ρ.

All conclusions presented in this paper result from properties of many-particle systems (here an analogy to nuclear physics), thermodynamic considerations (temperature uniquely defined under solely thermal equilibrium) and from an analogues to standard, multi-component heat transfer principles (solid conduction plus radiation in thin films).

8 References

1 Wilson M N, Superconducting Magnets, in: Scurlock, R. G. (Ed.) Monographs on cryogenics, Oxford University Press, New York, reprinted paperback (1989)

2 Dresner, L.: Stability of Superconductors, in: Wolf St. (Ed.) Selected topics in superconductivity, Plenum Press, New York (1995)

3 Seeger, B. (Ed.), Handbook of Applied Superconductivity, Vol. 1, Institute of Physics Publishing, Bristol and Philadelphia, IOP Publishing Ltd (1998)

4 Reiss H, Finite element simulation of temperature and current distribution in a superconductor, and a cell model for flux flow resistivity – Interim results, J. Supercond. Nov. Magn. **29** (2016) 1405 – 1422

5 Reiss H, Stability of a (2G) Coated, Thin Film YBaCuO 123 Superconductor - Intermediate Summary, J. Supercond. Nov. Magn. **33** (2020) 3279 - 3311

6 Reiss H, An Attempt to Improve Understanding of the Physics behind Superconductor Phase Transitions and Stability, http://arxiv.org/abs/2102.05944 (2021), accepted for publication in Cryogenics (2021), in production (2022)

7 Reiss H, A microscopic model of superconductor stability, J. Supercond. Nov. Magn. **26** (2013) 593 - 617

8 Reiss H, Stability considerations using a microscopic stability model applied to a 2G thin film coated superconductor, J. Supercond. Nov. Magn. **31** (2018) 959 - 979

9 Phelan P E, Flik M I, Tien C L, Radiative properties of superconducting Y-Ba-Cu-O thin films, Journal of Heat Transfer, Transacts. ASME 113 (1991) 487 – 493

10 Buckel W, Kleiner R, Superconductivity, Fundamentals and Applications, Wiley-VCH Verlag, 2nd Ed. Transl. of the 6th German Ed. by R. Huebener (2004)

11 Gray K E, Long K R, Adkins C J, Measurements of the liftime of excitations in superconducting aluminium, The Philosophical Magazine 20\50164\5 (1969) 273 - 278

12 Gray K E, Steady state measurements of the quasiparticle lifetime in superconducting aluminium, J. Phys. F: Metal Phys. (1971, Vol. 1) 290 - 308

13 Annett J, Superconductivity, Superfluids and Condensates, Oxford Master Series in Condensed Matter Physics, Oxford University Press (2004)

14 Köbler U, Bose-Einstein Condensation of Cooper-Pairs in the conventional superconductors, Int. J. Thermophys. (IJoT) **24** (3) (2021) 238 - 246

15 Kadin A M, Spatial structure of the Cooper Pairs, J. Supercond. Nov. Magn. **20** (4) (May 2007) 285 - 298

16 Glover III R E, Superconductivity above the transition temperature, in: Gorter C J (Ed.), Progress in low temperature physics, Vol. VI, Chap. 7, North-Holland Publishing Company, Amsterdam, London (1970) 291 - 332

17 Russell, H W, Principles of Heat Flow in Porous Insulators, J. Am. Ceram. Soc. **18** (1935) 1 - 5

18 Reiss H, Relaxation and a non-local, resistivity boundary layer in superconductors, arXiv 2202.04408 (Febr 2022)

19 Reiss H, Radiative Transfer, Non-Transparency, Stability against Quench in Superconductors and their Correlations, J. Supercond. Nov. Magn. **32** (2019) 1529 - 1569

20 Poole, Jr. Ch P, Datta T, Farach H A, Copper oxide superconductors, J. Wiley & Sons, Inc., 1988

21 Reiss H, The Additive Approximation for Heat Transfer and for Stability Calculations in a Multi-filamentary Superconductor - Part A, J. Supercond. Nov. Magn. **32** (2019) 3457 - 3472; Part B, J. Supercond. Nov. Magn **33** (2020) 629 - 660

22 Reiss H, Wärmestahlung - Superisolierungen, in: Stephan P et al. (Eds), VDI Wärmeatlas (German VDI Heat Atlas), Springer Verlag, 12th Ed. (2021)

Appendix

Figure 9 illustrates the applied symmetry operations. First, two operations, $\rho_{El,SC}(T) \rightarrow \rho_{El,SC}(-T)$, with the vertical axis T_{Crit} = const as the mirror plane, and $\rho_{El,SC}(-T) \rightarrow -\rho_{El,SC}(-T)$, with the vertical position of the mirror plane defined by the solid red circle (the maximum obtainable in the calculations of the resistivity in quadrant IV or III). These steps are followed by $-\rho_{El,SC}(-T) \rightarrow -\rho_{El,SC}(-T) + |\Delta\rho_{El,SC}(-T)|$. In total, all these operations simulate a point-symmetry operation of $\rho_{El,SC}(T)$ against the solid, red circle.

The linear transformation $-\rho_{El,SC}(-T) \rightarrow -\rho_{El,SC}(-T) + |\Delta\rho_{El,SC}(-T)|$, from quadrant II to quadrant I using the constant $|\Delta\rho_{El,SC}(-T)|$ serves to adjust the final $\rho_{El,SC}(T)$ in quadrant I to overlap with the normal resistivity of the superconductor, $\rho_{El,SC}(T)$, at $T \geq T_{Crit}$ (the solid, light-blue circles in Figure 9).

The limit which is set to the approximation of $\rho_{El,SC}(T< T_{Crit})$ to the normal conduction $\rho_{El,NC}(T \geq T_{Crit})$ is given by the numerically obtainable maximum $\rho_{El,SC}(T < T_{Crit}) = \rho_{El,SC}(T = T')$. The maximum follows from limitations (maximum number of digits of integer and real type variables) experienced when temperature shall approach T_{Crit} as close as possible. The final difference $\rho_{El,SC}(T= T') - \rho_{El,NC}(T \geq T_{Crit})$ is applied as a linear shift, $|\Delta\rho_{El,SC}(-T)|$, of the curve $\rho_{El,SC}(T)$ when it is mapped from quadrant II to quadrant I.

Figures

(a) Figures in Manuscript

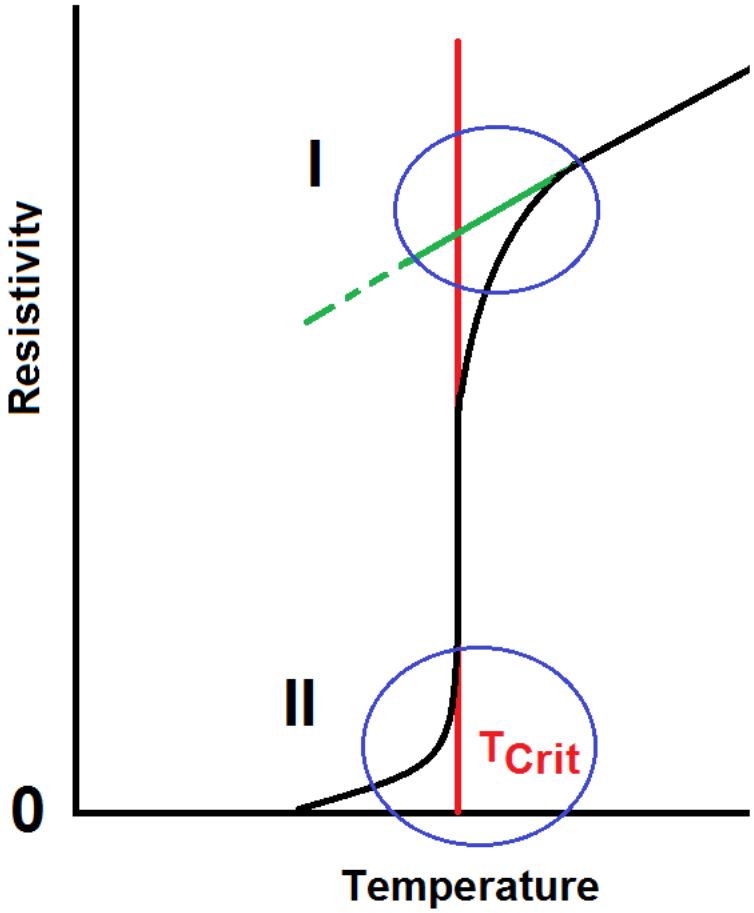

Figure 1 Resistivity, $\rho_{El}(T)$, of superconductors near critical temperature (schematic). For examples see e. g. Figure VII - 11 in the book "Copper Oxide Superconductors" by Poole, Datta and Farach [20] that shows bending of the resistivity vs. temperature curves of YBaCuO 123 and of other superconductor compounds in which a Rare Earth element has been substituted for the element Y in the $REBaCuO_{7-x}$ family. At T_{Crit}, the coloured, open ellipses I and II highlight well-known deviations from the sharp increase of $\rho_{El}(T)$ usually expected during a warm-up (in this Figure, the deviations are exaggerated). Meaning of the green solid line attached to the resistivity curve at $T > T_{Crit}$ is explained in Sect. 6.2.

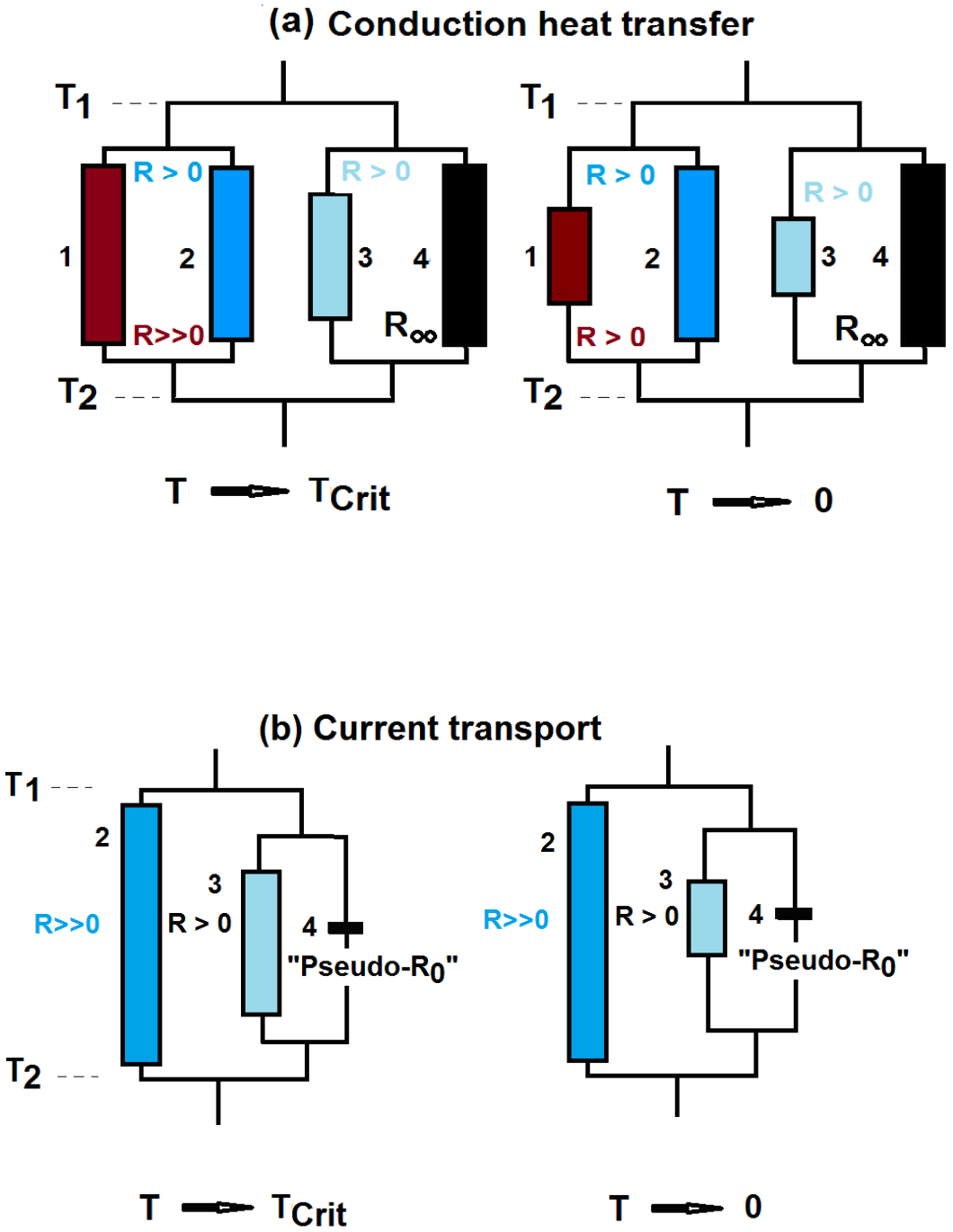

Figure 2a,b Resistance networks: (a) thermal and (b) electrical resistances, all at $T < T_{Crit}$. The diagrams are used to specify application of the Russell cell model [17] for thermal and electrical conduction transport in a superconductor (schematic, strongly simplified). The percentage of electrons (of the *total* body) that are available ("active") for thermal and electrical transfer applies to the composite of resistances 3 (light-blue) and 4 (black) in both diagrams (a) and (b). The dark-blue rectangles denote the single (not condensed to pairs) electron contribution to resistance of the *residual*

body, and the brown rectangles denote the thermal resistance by the lattice (phonons).

(a) Conduction heat transfer at different temperature. Dark brown and ark-blue thermal rectangles indicate non-zero phonon and single electron *thermal* resistances, (1) R_{Ph}, (2) and (3) R_{El}, respectively. The black resistance (4) R_{∞}, applies to electron pairs and illustrates their infinitely large thermal resistance (regardless of their number). Their zero contribution to conduction heat transfer results from vanishing collisions with the lattice. Vertical length of the black rectangles schematically indicates increasing number of electron pairs. At very low temperature, heat transfer in both (a) and (b) being subject to resistances $R_{Ph} > R_{El}$, the thermal conductivity of the superconductor to the most part is by single (not condensed) electrons. Under given temperatures, T_1 and T_2, solution of Fourier's differential equation yields the phonon temperature within resistance 1 that, at any co-ordinate, is different from electron temperature in resistances 2 and 3, in particular if coupling between electrons and lattice is weak. Temperature of channel 3 like channels 1 and 2 is below T_{Crit} but otherwise undetermined.

(b) Current transport, like in (a) at different temperature (again schematic, strongly simplified). Against (a), dark-brown rectangles (1) are cancelled (totally insulating, electrical transport channel). Single (not condensed) electrons contribute, according to non-zero, electrical resistances, R_{Ph} and R_{El}, respectively. The black rectangles (resistances R_o) illustrate zero resistance of electron pairs. Regardless of their number, total contribution to current transport is by electron pairs only. In order to make the Russell cell model (as a conduction or resistance model) applicable for the simulations, an at least 20 orders of magnitude smaller electrical resistance, in relation to normal electrical conduction, has to be assumed (this is schematically indicated by the small, non-zero vertical length of the black rectangles).

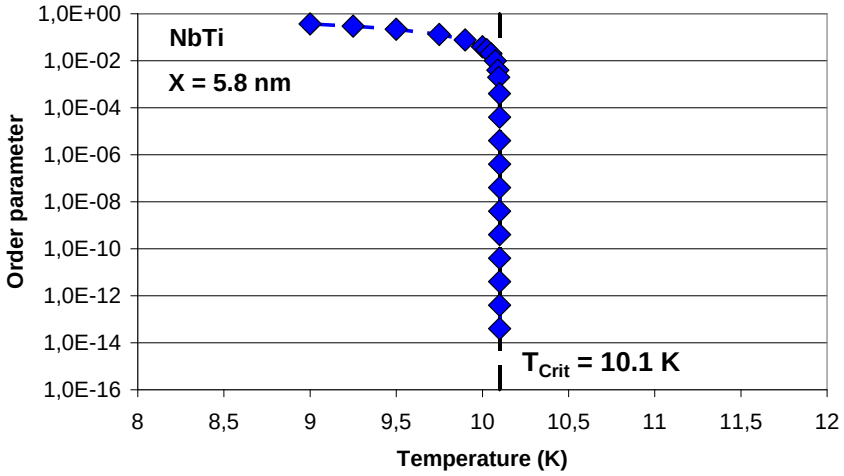

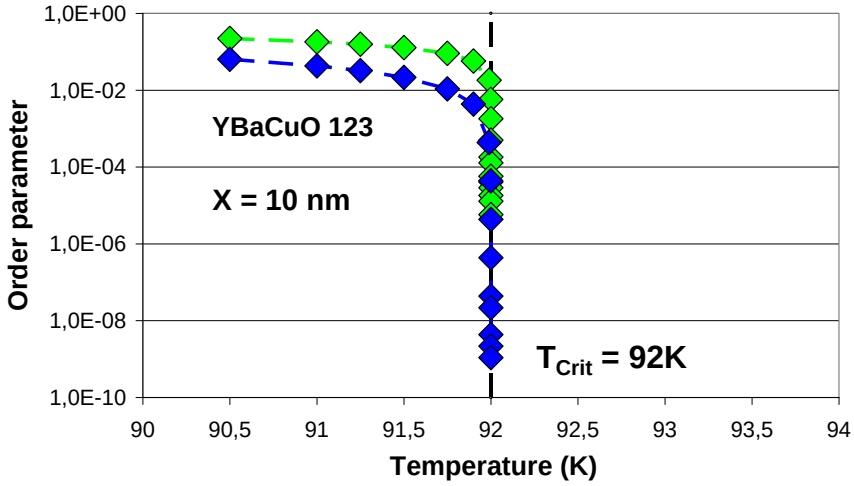

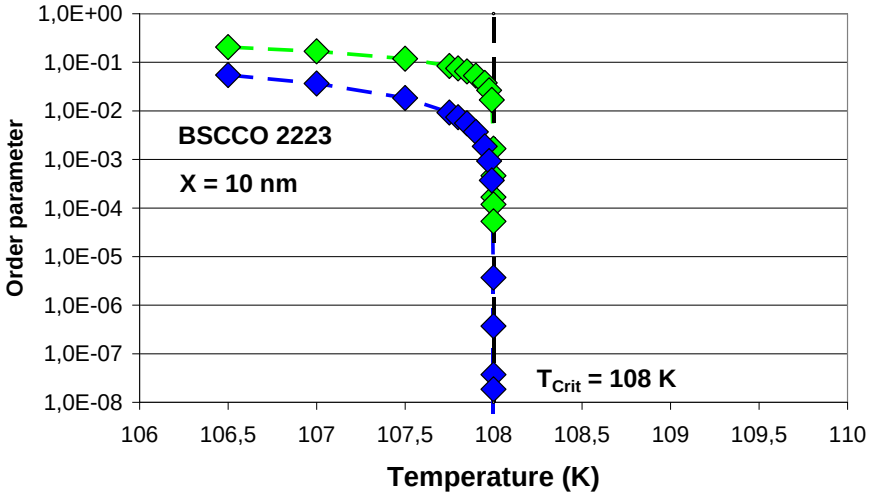

Figure 3 Order parameter, $f_S = n_S(T)/n_S(T=4K)$ of NbTi, YBaCuO 123 and BSCCO 2223 vs. temperature. Results are obtained using either the microstability model [7] or the approximation Eq. (8) of [9] (light-green and blue symbols, respectively).

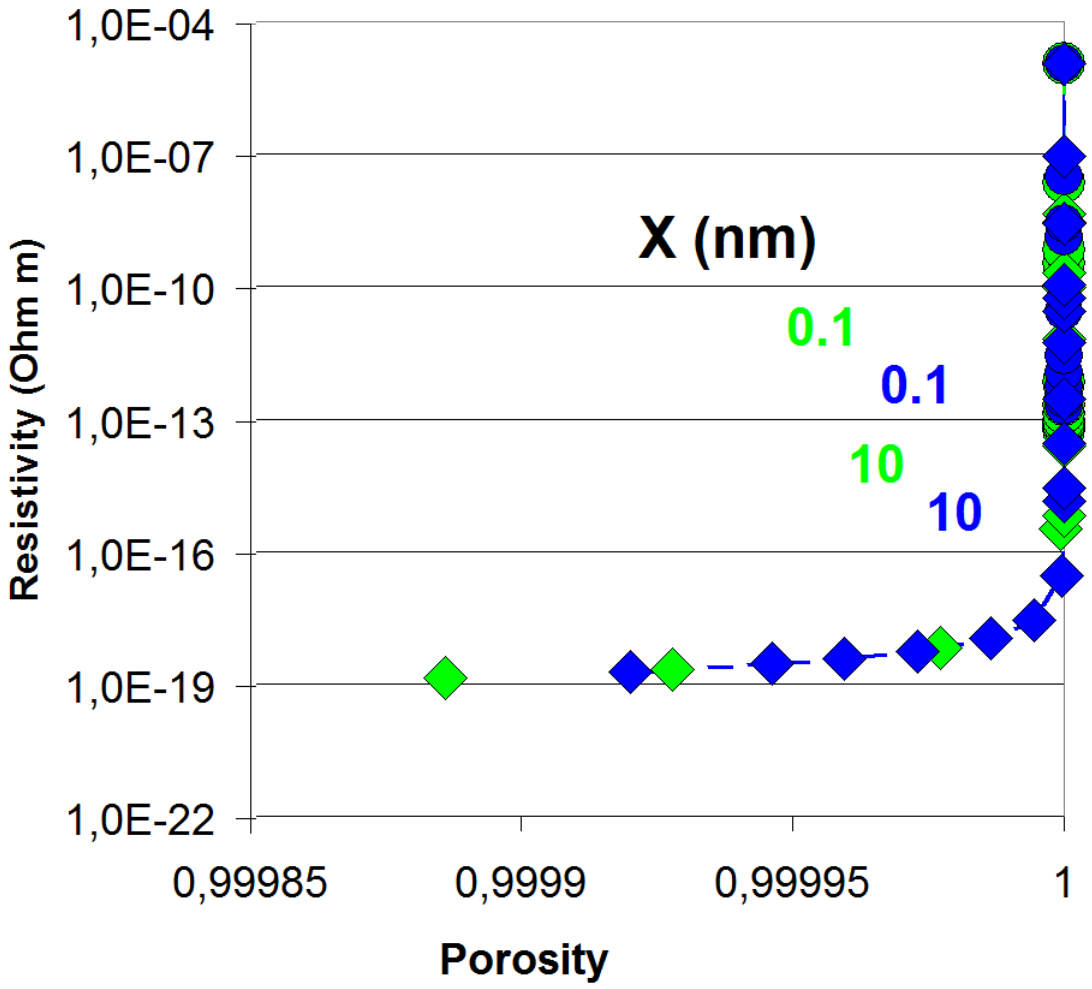

Figure 4 Dependence of the resistivity, $\rho_{El,SC}$, on porosity of YBaCuO 123 (using different coherence lengths, X (light-green and blue symbols). The calculations, to obtain order parameter, f_S (Figure 3), porosity, Π, and resistivity, $\rho_{El,SC}$, apply the microscopic stability model ([7], solid diamonds) or the approximation Eq. (8) of [9] (solid circles), respectively. Under increasing temperature, all curves, Π,) and $\rho_{El}(T)$, steadily converge to Π = 1 and to $\rho_{El,NC}$ (the normal conduction value), respectively. The sharp increase of the resistivity is due to the results found for the order parameter.

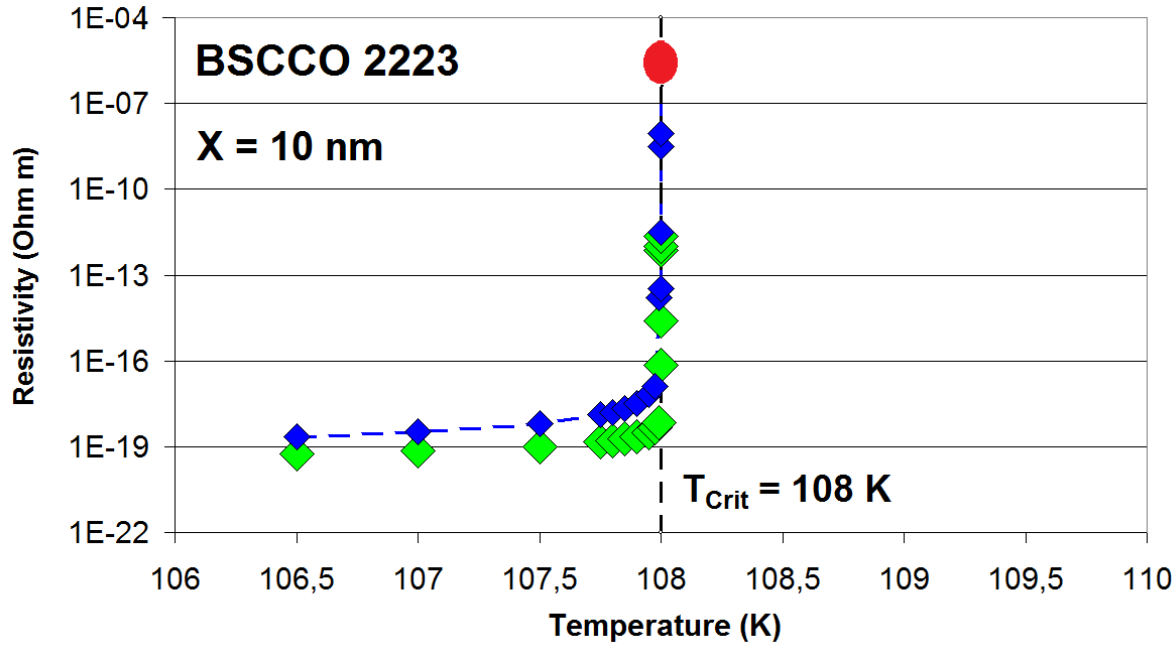

Figure 5 Effective electrical resistivity, $\rho_{El}(T)$, of BSCCO 2223 near phase transition. The results are obtained *before* point-symmetry operations (see text and Appendix) have been performed. The curves are obtained using the Russell cell model [17], with order parameter, $f_S(T)$, and porosity, Π, either from application of the microscopic stability model [7] (light-green) or from application of the approximation (Eq. (8) in [9] (blue, solid diamonds). The value of the superconductor pseudo-conductivity, $\rho_{el,SC}$,amounts to 10^{-25} Ω m. Curvature of $\rho_{El}(T)$ below T_{Crit} is confirmed, for any variations of $\rho_{El,SC}$ between this value and 10^{-50} Ω m. Meaning of the red solid circle is explained in Figure 9 in the Appendix. Note the logarithmic scale of the resistivity axis.

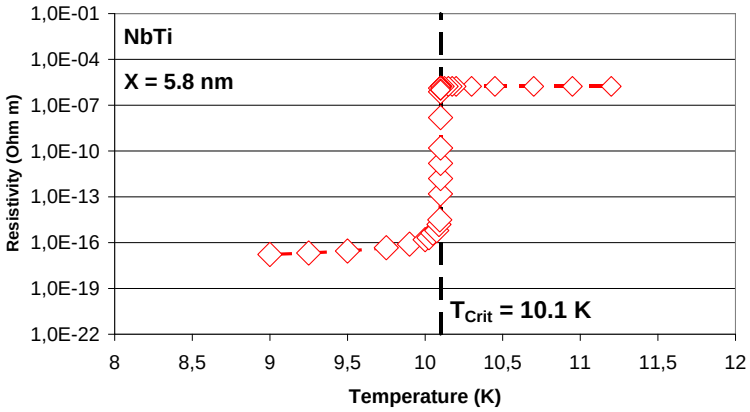

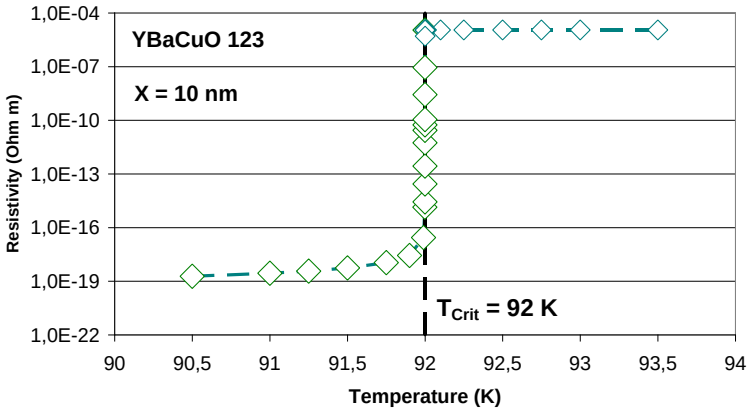

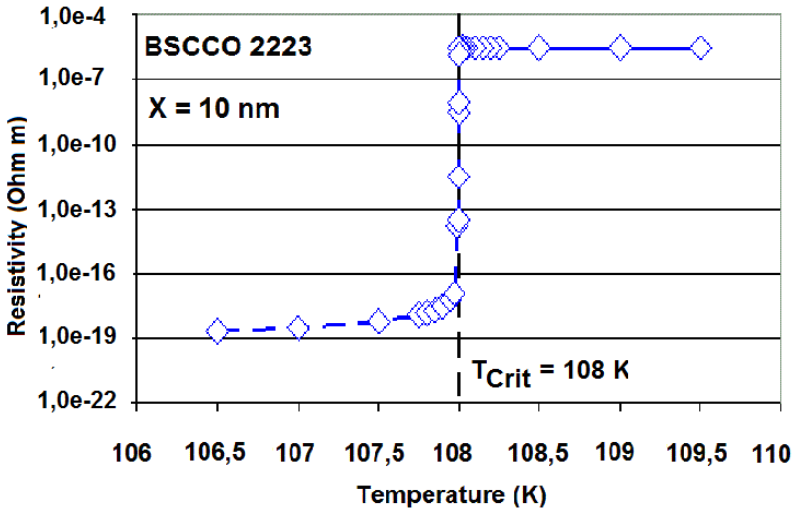

Figure 6a Resistivity vs. temperature, the "full curves" obtained *after* completion of the point-symmetry operation (extended to quadrant I) onto the results calculated for the NbTi, YBaCuO 123 and BSCCO 2223 superconductors (the procedure follows Figure 9 in the Appendix). While in the region $T < T_{Crit}$, between 10^{-19} and 10^{-13} Ω m, bending of the curves near 108 K is clearly seen, it cannot be revolved to the same extent between 10^{-7} and 10^{-4} Ω m because of the logarithmic resistivity scale. Open

symbols are applied to improve visibility of the curvatures under logarithmic resistivity scales; these are seen more clearly if the conductivity, instead of the resistivity, is considered, compare Figure 6c).

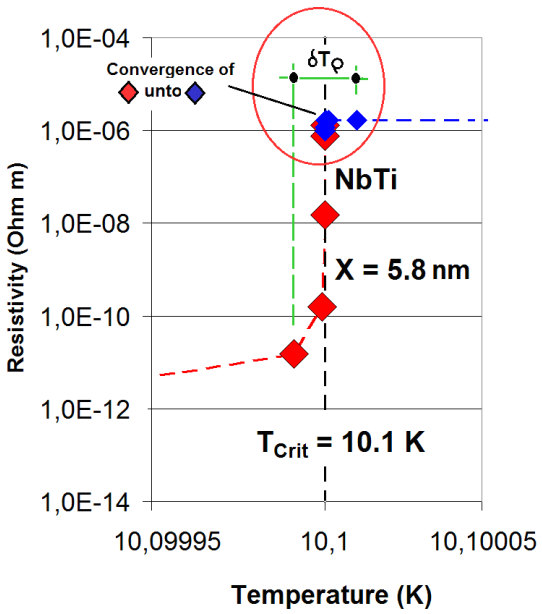
1,0E-04
1,0E-06
1,0E-08
1,0E-10
1,0E-12
1,0E-14
Resistivity (Ohm m)
Convergence of
unto
δTc
NbTi
X = 5.8 nm
TCrit = 10.1 K
10,09995
10,1
10,10005
Temperature (K)

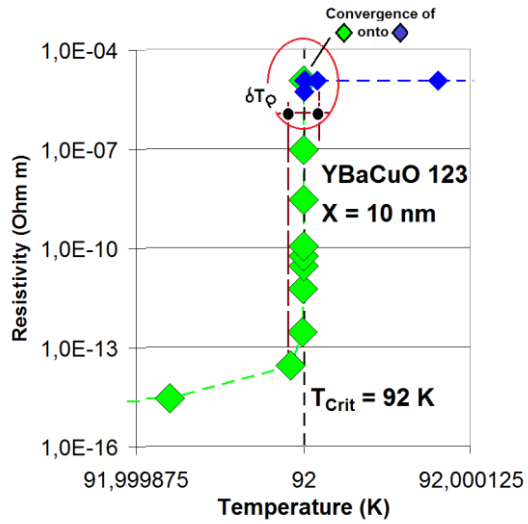
Convergence of
onto
1,0E-04
1,0E-07
1,0E-10
1,0E-13
1,0E-16
Resistivity (Ohm m)
δTc
YBaCuO 123
X = 10 nm
TCrit = 92 K
91,999875
92
92,000125
Temperature (K)

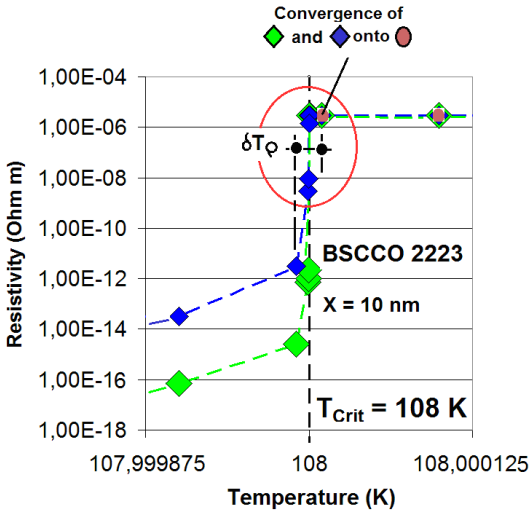
Convergence of
and
onto
1,00E-04
1,00E-06
1,00E-08
1,00E-10
1,00E-12
1,00E-14
1,00E-16
1,00E-18
Resistivity (Ohm m)
δTc
BSCCO 2223
X = 10 nm
TCrit = 108 K
107,999875
108
108,000125
Temperature (K)

Figure 6b Details of the resistivity vs. temperature curves of NbTi, YBaCuO 123 and BSCCO 2223 obtained after completion of the point-symmetry operations extended to quadrant I (see text and Figure 9 for explanation). The horizontal temperature scale is strongly magnified. All diamonds converge to the normal conduction resistivity, $\rho_{El,NC}$, at $T > T_{Crit}$ (the light-brown, solid circles in the bottom diagram) of the superconductor. The Figure shows, very close to T_{Crit}, the non-local, resistivity boundary layer expressed as the temperature uncertainty, δT_{ρ} in the three materials.

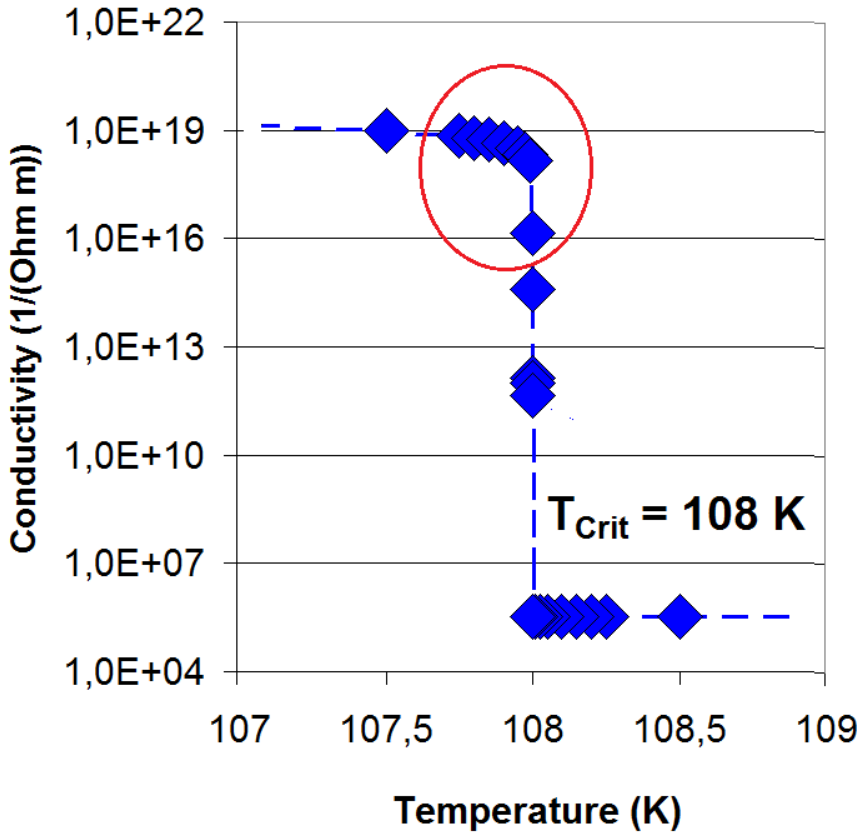

Figure 6c Electrical conductivity, $1/\rho_{El,SC}$, of BSCCO 2223 calculated from the resistivity values shown in Figure 6a. The red circle highlights bending of the curve that here is more clearly seen than in Figure 6a,b.

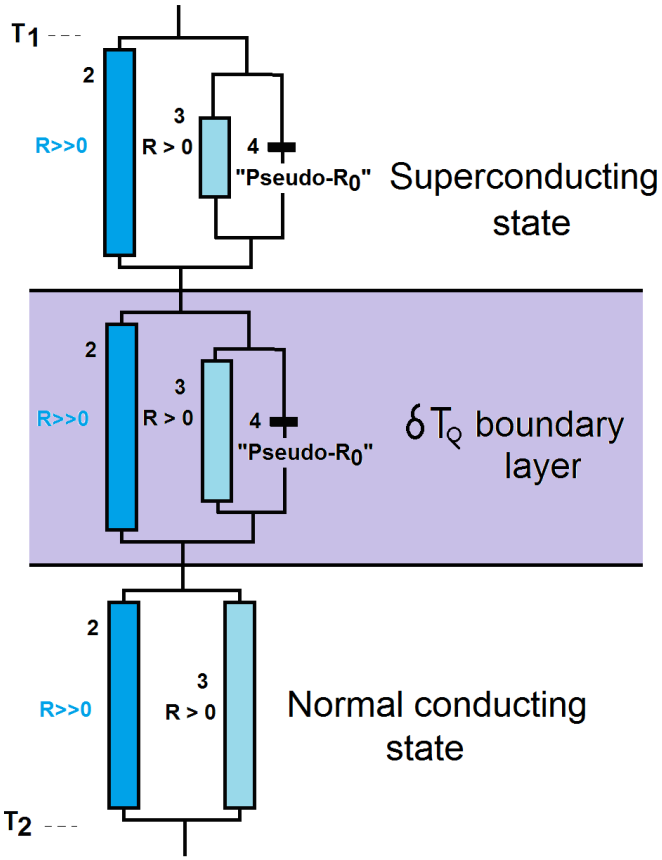

Figure 7 Resistances of a stack of thin films (schematic) with solid/solid contacts. The Figure, from top to bottom, simulates a standard, superconductor/normal conductor/superconductor sequence. For the simulation of Andreev reflection, layer 2 (mid-position) is normal conducting. Transition from superconducting to normal conducting resistivity is indicated by a ϑT_ρ resistive boundary layer, a temperature uncertainty extending over given geometrical layer thickness. Compare text.

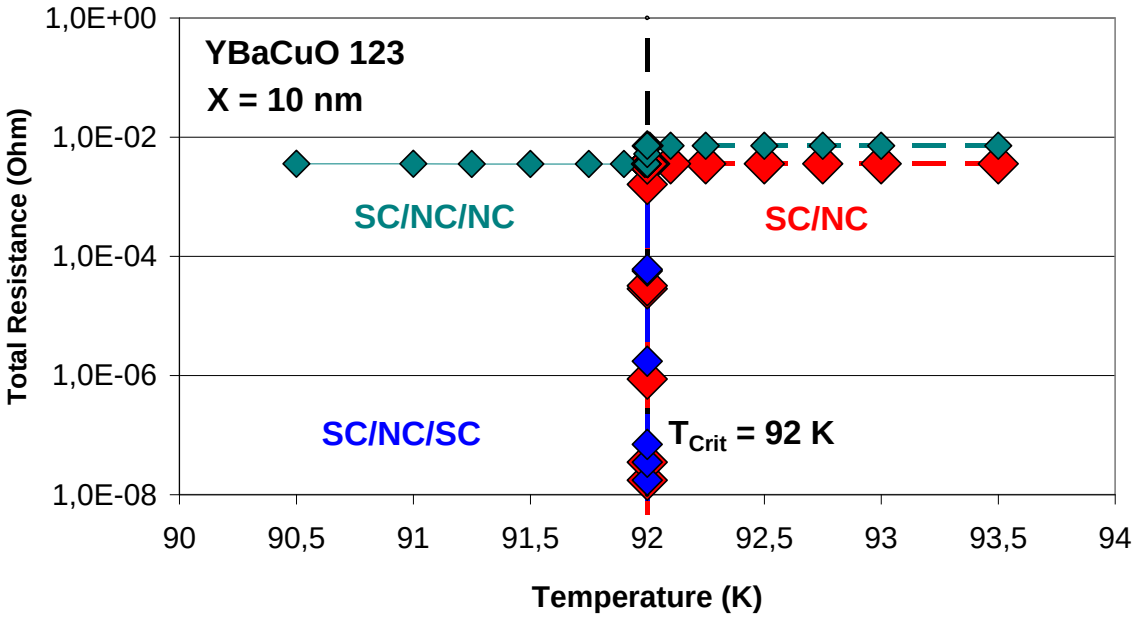

Figure 8 Total (serial) resistances of the stack shown in Figure 7 consisting of three layers of *identical* superconductor material (YBaCuO 123) but in different thermodynamic states that are identified by their pseudo-porosity. Thickness of the thin films is 10/0.01/10 µm, cross section is 10^{-4} m^2. It is clear the thickness of 10 µm is by a factor of 3 - 5 too large for achieving optimum results with (2G) thin film YBaCuO superconductors, but has been chosen to allow better comparison of the results obtained for the three layer combinations. Andreev reflection (the three layer sequence SC/NC/NC, green diamonds) effectively it is a SC/NC sequence. SC/NC (red diamonds) simulates a standard superconducting/normal conducting materials sequence of only two thin films. The resistances of SC/NC/NC and SC/NC cannot be identical due to the larger thickness of the SC/NC/NC sequence.

(b) Figures in the Appendix

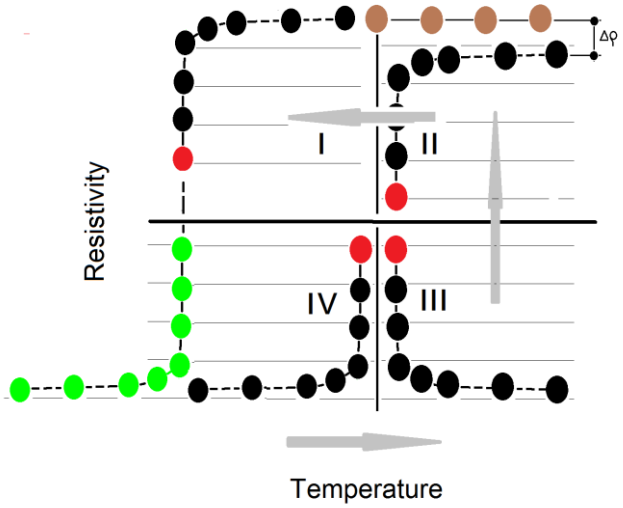

Figure 9 Stepwise explanation of point symmetry (mapping) of the $\rho_{El,SC} = f(T)$, here indicated by solid, black circles (schematic). The symmetry operation starts in quadrant IV with the $\rho_{El,SC}$ shown in Figure 5. The red, solid circle denotes the maximum value obtained in the series $\rho_{El,SC} = f(T)$, in this quadrant. Mapping is continued (light-grey arrows) counter-clock wise to the final result seen in quadrant I (the real values are shown in Figure 6a). The light-brown, solid circles denote the normal conduction resistivity, $\rho_{El,NC}$, of the superconductor. See text for more explanations.

Supporting Information

Supporting Information 1 (The microscopic stability model)

Some additional information on this model is given and some of its consequences are summarized.

(a) After completion of the relaxation, the model allows to calculate the total time needed to arrive at a new, dynamic equilibrium. This requests calculation how long it takes a single (of a very large number) of decay and recombination processes to be completed,

(b) a “time of flight”-concept with a mediating Boson. In nuclear physics, the Yukawa-model (as one of various analogues), a pion, π, mediates coupling (binding) of two nucleons, like the n and p in a Deuteron,

(c) the Pauli selection rule, and (d) the uncertainty principle.

The following conclusion, to be drawn from this model, is inevitable, for simply thermodynamic reasons, and it is absolutely contrary to standard understanding of critical temperature:

If T_{Crit} exists, it can be understood as being either

- a rough description of a thermodynamic *non-equilibrium electron* state (this is a standard but only approximate interpretation), which means: From purely thermodynamic standpoints, T_{Crit} cannot be explained as a thermodynamic temperature of *uniquely* defined value,
- or T_{Crit} correlates, as a thermodynamic *equilibrium* variable, with a corresponding, completed (which means, really existing, final)

dynamic equilibrium electron state. The prediction from [7] is that in this case the new equilibrium electron state cannot be reached within finite (reasonably extended) process or simulation time.

Beginning with a start temperature, conservation of energy during warm-up requests a temperature increase, T' > T. This concerns a fraction of the total electron body (electrons available, i. e. active in this warm-up process). The fraction depends on materials properties of the superconductor, temperature range (high-T_c or LHe-cooled?), interactions with the lattice and binding and energy states. The fraction is indicated in the literature, for low-T_C and high-T_C superconductors, as roughly 0.1 and 10 percent of the total number of electrons, respectively; experimental data cannot be found. But it is the *principle* (the balance) that is to be observed: Reorganisation of *this* fraction of electrons, regardless of the real percentage of the whole body, and not only a limited number that, for example, might be available from injection experiments.

The question is not only whether critical temperature can be *measured* precisely, with vanishing error bars. In superconductors it is instead the uniquely defined *existence* of critical temperature that has to be verified. Existence of a uniquely defined T_{Crit} depends on the thermodynamic state of the superconductor electron system.

Critical temperature may be hidden, be out of sight during finite, experimental or simulated periods of time, from observation. Critical temperature, if it is understood as a *sharply defined quantity*, therefore most probably is a fiction. It is not *an observable* that exactly describes a phase transition occurring simultaneously and uniformly in the superconductor volume.

This conclusion is supported by results from an alternative explanation of the bending observed in the resistivity, $\rho_{El}(T)$ and apparently also in the thermal fluctuations effects, see Sects. 3 and 4 of the present paper. There an uncertainty temperature interval, in the resistivity vs. temperature diagram, is reflected by a non-local layer, δT_{ρ} (Figure 6b).

Critical temperature thus is not a uniquely (sharply) defined quantity but, as a *limes* of a sequence of intermediate, non-equilibrium states, is embedded in a finite, very small temperature *interval within which* events and their distance from the phase transition can be studied.

Calculations of transient temperature distributions, stability against quench and existence of a non-local boundary layer, can safely be performed, strictly speaking, *only if* a *convergence limes* of a series would exist within which T steadily approaches T_{Crit}. Practically, all decisions related to the superconductor/normal conductor phase transition are uncertain within the very small temperature interval δT_{ρ}.

Consequences from this conclusion should be observable in levitation experiments and standard measurements of critical current density the latter in dependence of time; they might not reflect completion to equilibrium. This means: no "macroscopic" equilibrium like stable levitation co-ordinate (a "mechanical" equilibrium) and no stable final value of J_{Crit} would be observed. This is because a "microscopic" dynamic equilibrium, on the atomic level, might not be obtainable within reasonable time scales. It would be very interesting to see long-time measurements of levitation co-ordinates or or long-time measurements of J_{Crit} that are performed under absolutely stable temperature conditions.